

B 12 Dynamics of Glass Forming Systems

R. Zorn

Institut für Festkörperforschung

Forschungszentrum Jülich GmbH

Contents

1	Introduction	2
1.1	Phenomenology of glass forming materials	2
1.2	Theories and models	4
2	Simulation of a glass forming system	7
2.1	Kob-Andersen system, simulation technique	8
2.2	Mode-coupling interpretation	9
2.3	Dynamical heterogeneity	12
2.4	Confinement effects	17
3	Summary	20

1 Introduction

Glass formation, i.e. the solidification of a liquid without forming a crystal, is a very common phenomenon [1]. The range of materials forming glasses includes silicates (window glass), polymers (e.g. polystyrene), elements (Selenium), metals, biological materials and many more. From computer simulations it may even be speculated that any material vitrifies if it is cooled down sufficiently fast. Nevertheless, the glass transition and the related molecular dynamics are still poorly understood [2].

Although comparatively simple model systems and moderate particle numbers are sufficient to produce the signatures of the glass transition the use of computer simulation is rather new in this field. The reason is that the computational power required for such simulations is very high. As will be outlined in the following, systems approaching the glass transition show extremely long relaxation times. Therefore, a minimum of about 10^6 time steps is required to observe the characteristic dynamical features. In addition, the time for equilibration also increases dramatically.

Meanwhile, many glass forming systems have been studied by computer simulation. These can be roughly divided into two classes: (i) Simplified model systems for molecular glasses (e.g. [3]) or polymers (e.g. [4]): These models show the essential ('universal') features of glass forming materials. Due to their simplicity, it is possible to simulate long times up to about 100 ns. (ii) Molecularly or atomistically detailed models: The advantage of these is that they are fully comparable with real samples. They also show the non-universal particular features of a given molecular or polymeric system. So the resulting properties can be cross-checked with real experiments. On the other hand, the longest times in the simulation are much more restricted so that the general features of the glass transition cannot be studied as well.

In order to reasonably limit the scope, this lecture will only deal with one system of type (i) which was studied very thoroughly in the last decade. A 'realistic' polymer simulation of type (ii) is presented in another lecture (B.07, Richter).

1.1 Phenomenology of glass forming materials

Glass forming systems usually exhibit a plethora of dynamical phenomena, ranging from characteristic vibrations in the terahertz range to the structural relaxation which can take seconds or more. To discuss all these 'universal' dynamical features of amorphous materials (most of which are by now also studied by computer simulation) would exceed the scope of this lecture. Therefore, it will be restricted on the central and most important dynamical phenomenon in glass forming systems, the α relaxation. It is undisputed that any material which solidifies without crystallisation shows this type of dynamics with the characteristics listed in the following:

(1) Non-exponentiality. This feature is the longest-known in the history of glass research. Already in the 19th century Kohlrausch discovered [5] that the decay of the charge of a Leyden flask, a capacitor made from silica glass, is not exponential but can be described by the expression

$$\Phi(t) = \exp \left(-(t/\tau_K)^\beta \right) , \quad (1)$$

with $\beta < 1$. It is remarkable that this expression is used successfully till today in the description of various aspects of the dynamics of glasses. It applies as well to macroscopic quantities as the dynamic shear compliance [6] or the dynamic light scattering correlation function [7] as to microscopic correlation functions from neutron scattering [8].

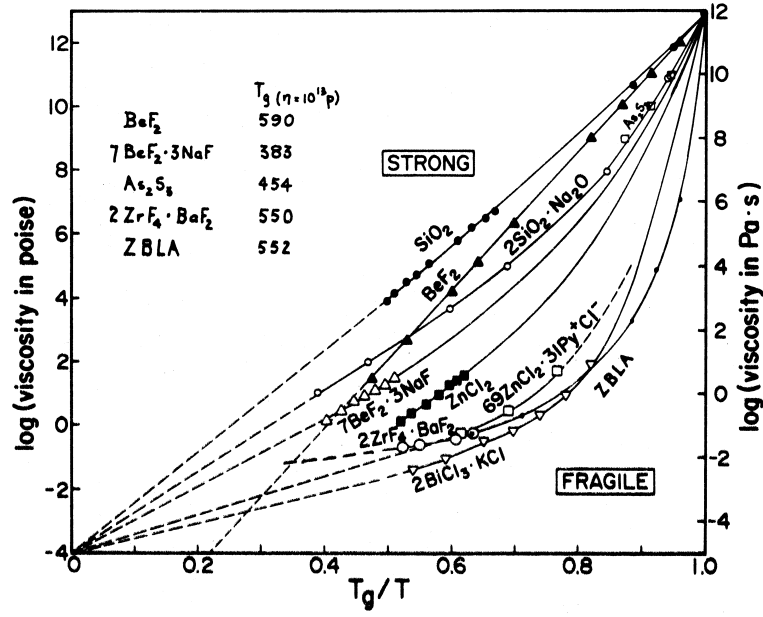


Fig. 1: Plot of logarithmic α relaxation times of various glass forming materials vs. the reciprocal temperature normalised to their respective glass temperature T_g , defined here as the temperature at which the viscosity $\eta(T_g) = 10^{12}$ Pas (equivalent to $\tau \approx 10^3$ s). [17]

The success of the ‘Kohlrausch law’ (1) is even more surprising considering that there is no theory that *exactly* predicts it. Mode coupling theory (MCT) [9] states it as limiting approximation to but not *the* solution of its dynamical equations [10]. The coupling model (CM) of Ngai [11] uses the expression only stating heuristic arguments for it. Approximately or asymptotically the Kohlrausch law could be derived for dynamics in fractal structures [12], fractal time [13], hierarchical models [14], or percolation models [15]. The special ubiquitous rôle of the form (1) may be related to its mathematical importance as the characteristic function of Levy’s stable distributions [16] but this property has never been exploited in a rigorous derivation but rather only as a motivation [13] of the widespread occurrence of the Kohlrausch law.

(2) Non-Arrhenius temperature dependence. Another characteristic feature distinguishing the α relaxation of glass forming materials from relaxations in ‘simple’ systems is the deviation of its temperature dependence from that expected for thermally activated processes, namely the Arrhenius law

$$\tau(T) \propto \exp(E_A/k_B T). \quad (2)$$

The degree of this deviation is very different for different glass forming materials leading to a classification by Angell [17, 18] into “strong” glasses following relation (2) closely to “fragile” ones which show a bent curve in the normalised activation plot $\log \tau$ vs. T_g/T [19, 17, 18] (Fig. 1).

The temperature dependence of the α relaxation can be described empirically by the Vogel-Fulcher [20, 21] expression

$$\tau(T) \propto \exp\left(\frac{A}{T - T_{VF}}\right). \quad (3)$$

At this point, a remark about the ‘glass transition’ in general is in order: Equation (3) suggests that there is complete vitrification at T_{VF} . This behaviour is experimentally unobservable because (i) most methods cease to be feasible for $\tau > 10^4$ s because of prohibitive experiment

duration¹, (ii) samples have to be equilibrated before the experiments and the time required for this (ageing time) increases in the same way as the α relaxation time τ itself. It is therefore not clear whether equation (3) holds up to the singularity, most recent experiments seem to negate this possibility [23]. For that reason the empirical dynamic glass ‘transition’ temperature T_g is defined as the temperature where $\tau(T_g) = 10 \dots 10^4$ s.

Also high precision measurements combined with an analysis of the derivatives of $\tau(T)$ show clear deviations from the VF expression (3) for high as well as low temperatures [24, 25]. Nevertheless, it seems to be an excellent description in an intermediate temperature range.

Empirically, a relation between non-exponentiality and non-Arrhenius temperature dependence can be found for glass forming [26] materials: ‘Fragile’ glasses seem to show a higher deviation from exponentiality.

(3) Time-temperature superposition principle. Despite being non-exponential the α relaxation usually exhibits the same shape over a large temperature range. This means that the relaxation of a quantity $\Phi(t)$ (e.g. the shear relaxation modulus $G(t)$) can be described by a master function Φ_α which is only rescaled to the individual temperatures:

$$\Phi(t, T) = \Phi_\alpha(t/\tau_\alpha(T)). \quad (4)$$

For the Kohlrausch expression (1) this means that β does not depend on temperature. This implies that the loss part of the susceptibility corresponding to the α relaxation obeys the inverse scaling law

$$\chi''(\omega, T) = \chi''_\alpha(\omega\tau_\alpha(T)). \quad (5)$$

This principle was first found from rheological measurements of the dynamic moduli [28]. It is still applied as a standard way to overcome the restricted dynamical range of such experiments. Measurements at different temperatures are spliced together to obtain a master curve which spans 12–14 decades.

The time-temperature superposition principle also applies to the microscopic dynamics seen in a neutron scattering experiment [8] (Fig. 2).

Nevertheless, experiments covering a large dynamical range by one technique show that deviations from time-temperature superposition occur. They can be detected in dielectric spectroscopy [29] as well as rheological measurements [6].

(4) α relaxation universality. Finally, the time scale $\tau(T)$ in general is the same for all relaxation processes—macroscopic (rheological, dielectric etc.) and microscopic. This can be recognised from Fig. 2: The fact that the (microscopic) relaxation curves from neutron scattering superimpose when the (macroscopic) shift factor from rheology [30] is used is by no means trivial. The former data reflects the loss of correlation on a length scale of $2\pi/q \approx 4$ Å while the latter is obtained from a macroscopic sample. This shows that there is indeed a universality of the α relaxation time scale covering all levels of motion from that of an individual molecular segment to the bulk. However, it should not be concealed that high resolution experiments show a deviation from the strict validity of the α relaxation universality.

1.2 Theories and models

In the last 50 years, a large number of theories and models has been devised to explain the features of the α relaxation (and related dynamical phenomena). Again, it is only possible to

¹ For an exceptional experiment of $2.5 \cdot 10^9$ s duration see [22].

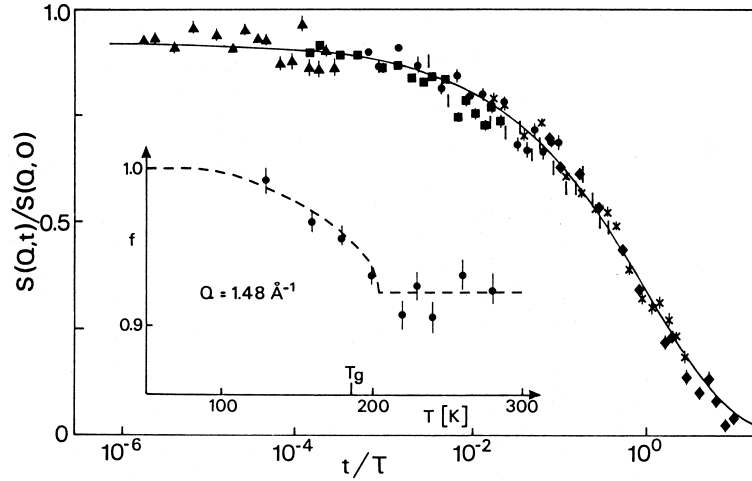


Fig. 2: Scaling representation of the neutron spin-echo data $S(q, t)$ from 1,4-polybutadiene at $q = 1.48 \text{ \AA}^{-1}$. (\blacktriangle , 200 K; \blacksquare , 220 K; \bullet , 230 K; $|$, 240 K; \times , 260 K; \blacklozenge , 280 K). The scale $\tau(T)$ is taken from a macroscopic viscosity measurement. Inset: Temperature dependence of the non-ergodicity parameter f_q . [8]

mention here two examples which are relevant to the discussion of the presented simulation results: the mode-coupling theory, which stimulated a lot of the interest in glass physics over the last 20 years, and the older model of cooperatively rearranging units which experienced a ‘revival’ due to recent simulation results.

(1) Mode-coupling theory. The only theory which is currently able to predict all mentioned features of the α relaxation from microscopic equations at least qualitatively is the mode-coupling theory (MCT) [9]. Time-temperature superposition and α relaxation universality follow directly from the mathematical properties of the MCT. Stretching is found, except for the simplest models of the MCT.

Starting point of MCT for structural glass formers is the normalised density-density correlation function:

$$F(q, t) = \frac{\langle \delta \varrho^*(q, 0) \delta \varrho(q, t) \rangle}{\langle \delta \varrho^*(q, 0) \delta \varrho(q, 0) \rangle}. \quad (6)$$

Here $\delta \varrho(q, t)$ are the Fourier components of the microscopic density fluctuations. For these components (modes) an infinite but closed set of equations of motion is established. This is done by simplifying the actual equations of motion using certain approximations [9]. It would exceed the scope of this lecture to discuss these approximations in detail but it has to be mentioned that they are plausible but uncontrolled. The MCT equations can be solved numerically (Fig. 3) or general scaling laws can be derived. The general form of the solution is a two-step relaxation. The general interpretation is that the first step is related to the ‘rattling’ motion of a particle (or a group of particles) in the cage formed by its neighbours while the second step represents its escape from the cage.

This second step is what in the experiment is observed as the α relaxation. For sufficiently long times the time-temperature superposition property

$$F(q, t, T) = \hat{F}(q, t/\tau_\alpha(T)) \quad (7)$$

can be derived within the approximations of MCT. The master function $\hat{F}(q, \hat{t})$ is non-universal

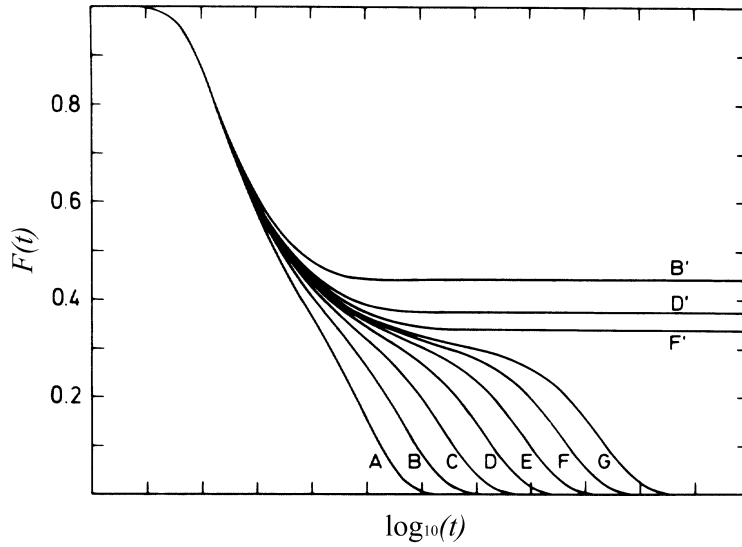


Fig. 3: Correlation function vs time from numerical solution of the MCT equations. The result here is shown for a schematic MCT model [31] with only a single mode but shows the same scaling and asymptotic properties as the full q dependent MCT. The curves A–G correspond to $T > T_c$, B'–F' to $T < T_c$ both approaching T_c with increasing index.

and depends on q . But it can be shown that the Kohlrausch expression (1) is a good approximation.

A strict ergodic to non-ergodic transition is predicted for a temperature T_c (which, as explained below, is higher than T_g). At this temperature the caging effect by neighbouring particles becomes so strong that a structural arrest occurs. This means that $F(q, t)$ does not decay to zero for $t \rightarrow \infty$ but to a finite value $f(q, T)$; there is no longer an α relaxation. Close to T_c the α relaxation time scale diverges with a power law

$$\tau_\alpha(T) \propto \epsilon^{-\gamma} \quad (8)$$

where $\epsilon = (T - T_c)/T_c$ with a high exponent $\gamma > 1.76 \dots$. Experimentally, such a power law can usually only be found in a small temperature region [24]. The extrapolated T_c is about 20% higher than the empirical glass temperature T_g . This is an indication of thermally activated ('hopping') processes which are only included in a more extended formulation of MCT [31]. These processes restore ergodicity even at temperatures below T_c where the 'ideal' MCT predicts a non-ergodic behaviour.

Several predictions of MCT focus on the crossover region between the first and the second step². In this regime a factorisation of the reduced correlator should be possible:

$$F(q, t) = f_c(q) + h(q) \sqrt{|\epsilon|} g(t/t_\epsilon). \quad (9)$$

Here, $f_c(q) = f(q, T_c)$ is the non-ergodicity parameter at T_c , $h(q)$ a positive amplitude factor, and $g(t)$ another master function. The ' β relaxation time scale' also follows a power law $t_\epsilon \propto |\epsilon|^{-1/2a}$ but with a smaller exponent.

² In MCT literature this is usually called the β relaxation. But it has to be noted that this terminology differs completely from that of experimental physics [32] where ' β relaxation' denotes a process which is orders of magnitude slower.

$g(\hat{t})$ depends on the microscopic details only via a single parameter λ . This parameter also determines the exponent a and another exponent b through the relation

$$\lambda = \frac{(\Gamma(1-a))^2}{\Gamma(1-2a)} = \frac{(\Gamma(1+b))^2}{\Gamma(1+2b)} \quad (10)$$

and in turn $\gamma = 1/2a + 1/2b$. $g(\hat{t})$ can be written as a series expression in \hat{t}^{-a} and \hat{t}^b . Asymptotically, it becomes

$$g(t/t_\epsilon) = (t_\epsilon/t)^a \quad (11)$$

for times $t < t_\epsilon$ and

$$g(t/t_\epsilon) = -B(t/t_\epsilon)^b \quad (12)$$

for times $t > t_\epsilon$ and $T > T_c$. The last relation implies that the incipient decay of the α relaxation is given by

$$F(q, t) = f_c(q) - \text{const} \cdot t^b. \quad (13)$$

This is the famous ‘von Schweidler’ law [33] which was proposed empirically also very early in the history of glass physics. It has to be noted that here b is not the exponent resulting from a series expression of the Kohlrausch function (1). Because the von Schweidler description holds for shorter times than the latter in general $b \neq \beta$.

(2) Cooperatively rearranging regions. As mentioned above one of the unsolved problems of the physics of glass forming materials is that the temperature dependence of relaxation times does not follow an Arrhenius law, i.e. plots like Fig. 1 show a curvature. In addition local fits with $\tau = \tau_0 \exp(E_A/k_B T)$ yield unphysically high values of the activation energy E_A and too short times for τ_0 . An early idea by Adam and Gibbs [34] (AG) to resolve this puzzle was that groups of z molecules (or monomeric segments for polymers) have to move at the same time to enable relaxation. If there is a minimum number z^* below which the molecules in a group block themselves it can be shown that the Arrhenius law changes into

$$\tau(T) = \tau_0 \exp(z^*(T)E_A/k_B T) \quad (14)$$

where now E_A is the activation energy for a single molecule [34]. In order to explain the positive curvature of Fig. 1 $z^*(T)$ has to be a decreasing function of temperature. This makes sense because one would expect a looser packing at high temperature and therefore the possibility for smaller groups to rearrange.

The groups considered here are usually called cooperatively rearranging regions (CRR) or -units. The problem with this kind of pictures is that the membership of a particle in a CRR needs not to have structural consequences. Experiments trying to detect density inhomogeneities on the length scale expected for the CRRs were until now futile. It may be that the CRRs can only be identified by their (faster) microscopic dynamics.

There are strong indications that glass forming liquids indeed show a microscopically heterogeneous dynamics [35]. Nevertheless, there are only few experiments allowing an unequivocal access to the spatial extent of the inhomogeneities, so that it is still unclear whether they correspond to the CRRs hypothesised.

2 Simulation of a glass forming system

As mentioned in the introduction computer simulations nowadays cover a large range of systems ranging from more abstract models to fully atomistic ones. So it is impossible to cover the field

in one lecture. For demonstration a single system is picked out here which has the advantage that many properties of it have been investigated. So it is only necessary to introduce the definition once in the first subsection. The further subsections will then always refer to the same (or only slightly modified) system.

2.1 Kob-Andersen system, simulation technique

The system presented here as an example is a binary mixture of particles A (80%) and B (20%) of the same mass m interacting by a Lennard-Jones potential

$$V_{\alpha\beta} = 4\epsilon_{\alpha\beta} \left((\sigma_{\alpha\beta}/r)^{12} - (\sigma_{\alpha\beta}/r)^6 \right) \quad (15)$$

where $\alpha, \beta \in \{A, B\}$ [3].

The reason for choosing a *mixture* is to avoid crystallisation. But it turns out that this is only successful for certain ‘irregular’ combinations of the parameters in expression (15), e.g. $\epsilon_{AA} = 1.0$, $\epsilon_{BB} = 0.5$, $\epsilon_{AB} = 1.5$, $\sigma_{AA} = 1.0$, $\sigma_{BB} = 0.88$, $\sigma_{AB} = 0.8$ ³. In the following all quantities will be expressed in terms of the parameters of the A particles, i.e. length in σ_{AA} , energy/temperature in ϵ_{AA} , and time in $\sqrt{m\sigma_{AA}^2/48\epsilon_{AA}}$. In analogy to argon these units correspond to a length of 3.4 Å, an energy of $k_B \cdot 120$ K, and a time of $3 \cdot 10^{-13}$ s.

The simulation was performed using the velocity form of the Verlet algorithm with a step size 0.01 for $T \geq 1.0$ and 0.02 for $T \leq 0.8$. The total number of particles was 1000–8000, the simulated volume a cubic box with periodic boundary conditions. The box size and thus the density was kept constant. In some but not all simulations it was adjusted before recording the trajectories to obtain the same pressure at all temperatures. So some of the results shown here correspond to isochoric lines (with often extremely high pressures) and some to isobaric lines of the phase diagram.

In order to probe equilibrium properties the systems were first kept at a high temperature ($T = 5$). Then, they were cooled down with rates decreasing with lowering the aimed-at temperature. For the lowest temperature ($T = 0.466$) a rate of $1.5 \cdot 10^{-7}$ was achieved, corresponding to $6 \cdot 10^7$ K/s in argon. This is still high compared to the rates used in experiments although it constitutes an improvement by an order of magnitude with respect to earlier simulations. To ensure that the systems were equilibrated, runs with different thermal history were compared and averaged. Further details of the simulations can be found in [3].

Fig. 4 shows the time development of the mean squared displacement

$$\langle r^2(t) \rangle = \frac{1}{N_A} \left\langle \sum_{i=1}^{N_A} |\mathbf{r}_i(t) - \mathbf{r}_i(0)|^2 \right\rangle \quad (16)$$

of the A particles for different temperatures. For short times $\langle r^2(t) \rangle$ is proportional to t^2 indicating a free-flight motion. For long times one finds $\langle r^2(t) \rangle = 6Dt$ characteristic for diffusive motion. For low temperatures a plateau around 0.04 develops. This means that the fast motion is blocked by the neighbouring particles as soon as it reaches a length scale of $\sqrt{0.04} = 0.2$ (in units of the particle diameter σ_{AA}). Only after a long time which for low temperatures can be orders of magnitude larger the particle can break out of the cage. So already from the simplest one-particle property, the mean squared displacement, the basic microscopic picture of MCT can be confirmed.

³ The parameter set is not chosen out of the blue but rather mimics the potential of the metallic glass Ni₈₀P₂₀.

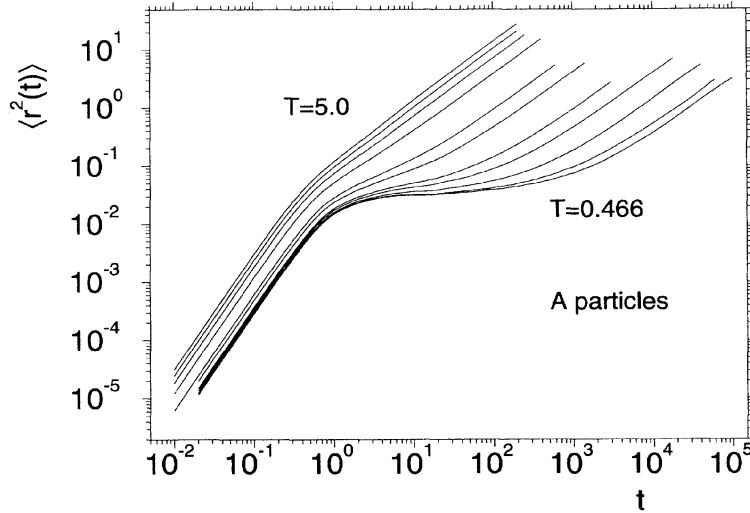


Fig. 4: Mean squared displacement for the A particles for all temperatures investigated in [3]: $T = 5, 4, 3, 2, 1, 0.8, 0.6, 0.55, 0.5, 0.475, 0.466$.

2.2 Mode-coupling interpretation

From the simulation results it is possible to calculate the normalised density correlation function (6) aka the coherent intermediate scattering function:

$$F(q, t) = \frac{\left\langle \frac{1}{N_A} \sum_{i=1}^{N_A} \sum_{j=1}^{N_A} \exp(i\mathbf{q} \cdot (\mathbf{r}_j(t) - \mathbf{r}_i(0))) \right\rangle}{\left\langle \frac{1}{N_A} \sum_{i=1}^{N_A} \sum_{j=1}^{N_A} \exp(i\mathbf{q} \cdot (\mathbf{r}_j(0) - \mathbf{r}_i(0))) \right\rangle} \quad (17)$$

From this quantity a direct test of MCT should be possible⁴. Fig. 5 shows a scaling plot, similar to Fig. 2, where $\tau(T)$ is the time where $F(q, \tau) = 1/e$ [37].

It can be seen that as soon as the two steps in $F(q, t)$ (corresponding to the two regimes observed in the mean square displacement) become distinct, the rescaled correlation functions fall onto one master curve. This means that the time-temperature superposition principle is fulfilled. Also in accordance with MCT the beginning ($t \lesssim \tau$) of the second step can be represented by the von Schweidler law (13). On the other hand the full MCT expression does not fit the data much better. Indeed, the time range of ‘critical decay’ $g(t) \propto t^{-a}$ cannot be found. The longer times can be fitted better with the Kohlrausch expression (1) but this is not in contradiction with MCT but rather what is expected for large q [38].

⁴ Actually, for any correlator of quantities having nonzero overlap with $\delta\rho(\mathbf{q}, t)$ the scaling properties of MCT should hold. Therefore, historically the first tests were done on the self part of (17) [36, 3], the *incoherent* intermediate scattering function

$$F_s(q, t) = \left\langle \frac{1}{N_A} \sum_{i=1}^{N_A} \exp(i\mathbf{q} \cdot (\mathbf{r}_i(t) - \mathbf{r}_i(0))) \right\rangle \quad (18)$$

In principle, this argument already has to be invoked when using the correlation function (17) because it only includes one combination of particles (here: AA) and therefore strictly speaking is different from the density-density correlator.

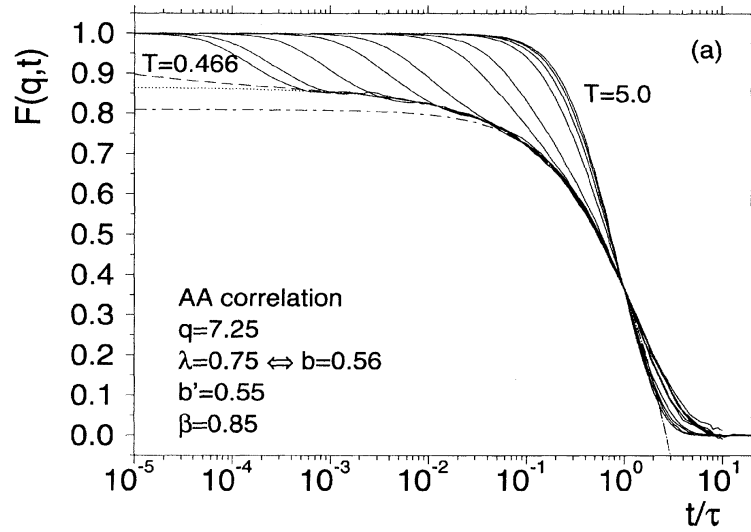


Fig. 5: Coherent intermediate scattering function $F(q, t)$ (solid lines) for all temperatures investigated in [37]. The dashed curve is a fit with a master curve proposed by MCT. The dotted curve is a fit with the von Schweidler law and the chain curve a fit with the Kohlrausch law.

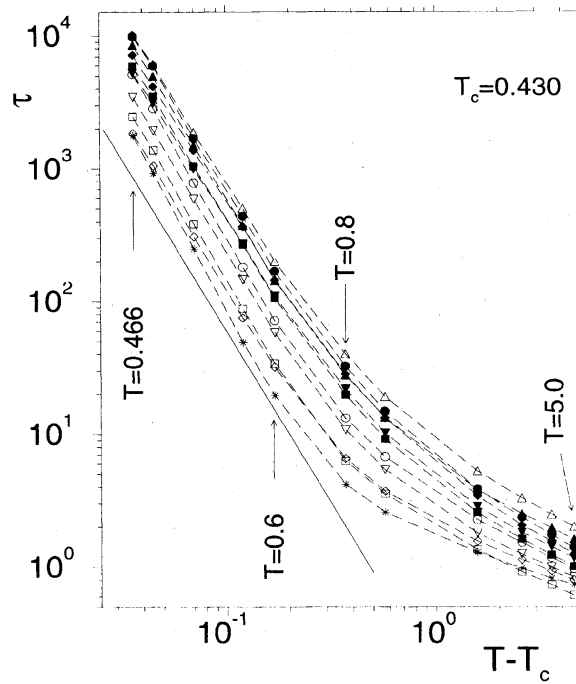


Fig. 6: Relaxation time τ vs temperature for various correlators. Squares and triangles pointing downwards: self correlation function $F_s(q, t)$ for A and B particles, respectively. Circles and diamonds: $F(q, t)$ for AA and BB correlation, respectively. Triangles pointing upwards and stars: $F(q, t)$ for AB correlation. Solid line: power law with exponent 2.6. From [37].

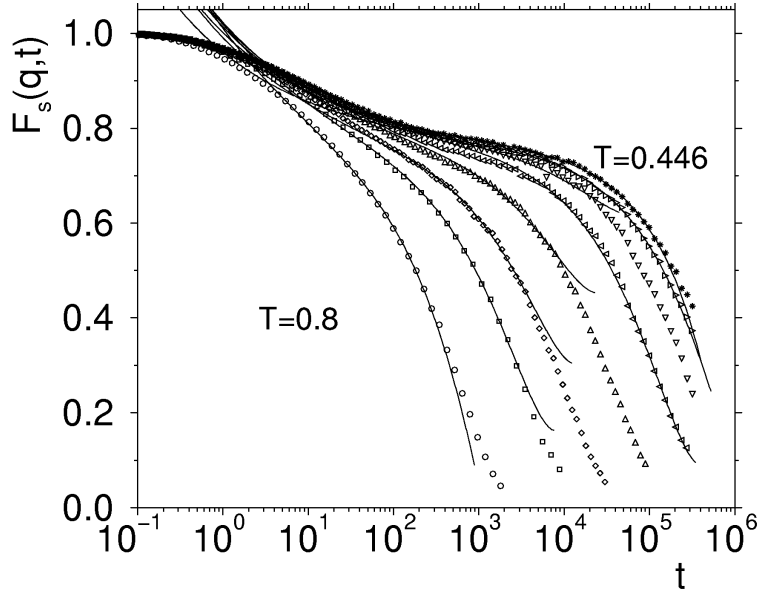


Fig. 7: Time dependence of $F_s(q, t)$ ($q = 7.2$) of the A particles for stochastic dynamics [40]. Temperatures: 0.8, 0.6, 0.55, 0.5, 0.475, 0.466, 0.452, 0.446. The solid curves are fits with the MCT expression (9).

According to MCT the scaling time should show a power law dependence on temperature, $\propto (T - T_c)^{-\gamma}$. As Fig. 6 shows this is fulfilled for a suitable choice of $T_c = 0.430$: The scaling times show this power law with $\gamma = 2.6$ for *all* correlators, i.e. also for the BB and AB counterparts of (17) and the self correlators. But here it has to be mentioned that the power law for the diffusion coefficient, $D \propto (T - T_c)^\gamma$, is obeyed only with a significantly different value of $\gamma = 1.7 \dots 2.0$ [36].

A characteristic feature of the MCT for structural glass formers is that quantities as $f_c(q)$, $h(q)$, and λ can all be calculated from the structure factor $S(q) = \langle \delta \varrho^*(q) \delta \varrho(q) \rangle$. This structure factor (here: the three structure factors for AA, BB, and AB correlations) can also be obtained from the simulation. The values of $f_c(q)$ and λ calculated in this way coincide well with the values from fitting the dynamical quantities except for the highest q [39].

As mentioned in the context of Fig. 5 the MCT expression (9) does not fit the simulation results well in the region where the asymptotics $g(\hat{t}) \sim t^{-a}$ should hold, the so-called ‘critical decay’. Another deviation can be found by analysing the dynamic susceptibility $\chi(q, \omega)$ which is the Fourier transform of $F(q, t)$ multiplied by ω . As predicted by MCT this quantity shows a minimum but this minimum does not show the predicted scaling properties $\chi_{\min} \propto \epsilon^{1/2}$ and $\omega_{\min} \propto \epsilon^{1/2a}$ [37]. This led to the suspicion that in the system studied here the β relaxation may be too much influenced by the long-time tail of the microscopic dynamics. In order to check this, a system with the same composition and potential was simulated with stochastic dynamics instead of Newtonian [40]. The stronger damping should avoid the distortion of the β scaling regime. Fig. 7 shows the results of such a simulation as the self correlator of the A particles together with fits with the MCT expression (9). The values f_c and h were fitted simultaneously, $g(\hat{t})$ calculated from MCT, and only t_ϵ fitted individually. It can be seen that the MCT expression fits much better here than for the Newtonian system. In addition, Fig. 8 shows that the timescale also follows the expected power law $t_\epsilon \propto \epsilon^{-1/2a}$.

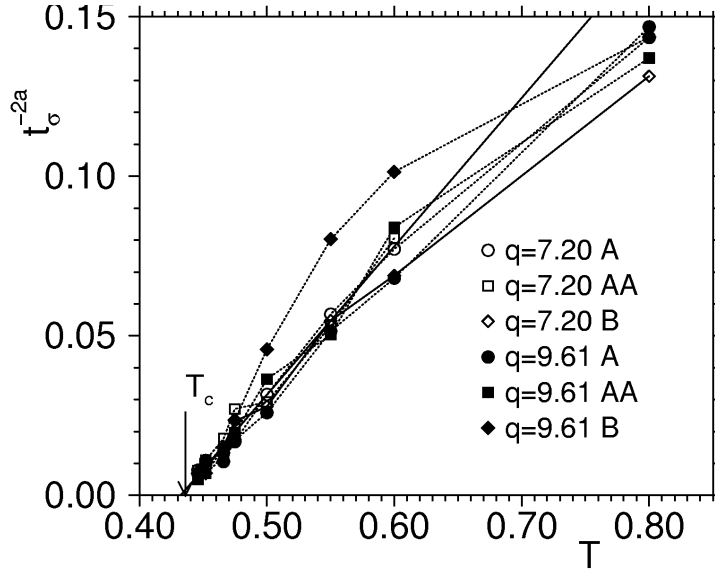


Fig. 8: Check of the validity of the power law scaling for the β relaxation $t_e \propto (T - T_c)^{-1/2a}$ for different correlators [40]. Temperatures: 0.8, 0.6, 0.55, 0.5, 0.475, 0.466, 0.452, 0.446.

2.3 Dynamical heterogeneity

The question of dynamical heterogeneity is currently strongly discussed in the physics of glass forming materials [35]. E.g. there are two fundamentally different explanations possible for a correlation function decaying with a ‘stretched’ law as (1): (i) There may be regions or even single particles with different relaxation times. Even if these individually relax according to an exponential law, by averaging one obtains $\Phi(t) = \int g(\tau) \exp(-(t/\tau)^\beta) d\tau$ where $g(\tau)$ is the distribution of relaxation times of the regions/particles⁵. (ii) The non-exponentiality could be an intrinsic property of the dynamics. In a real experiment it is difficult to distinguish both possibilities because it cannot be avoided to integrate over a large number of particles. The big advantage of computer simulation is here that individual particle trajectories are accessible.

(1) Non-Gaussianity. The most simple quantity giving an indication of dynamical heterogeneity can be derived from a cumulant expansion of the self correlator (18) [41]:

$$F_s(q, t) = \exp \left(-\frac{\langle r^2(t) \rangle}{6} q^2 + \frac{\alpha_2(t) (\langle r^2(t) \rangle)^2}{72} q^4 + \mathcal{O}(q^6) \right). \quad (19)$$

Here the non-Gaussianity parameter (nGP) is related to the momenta of the particle displacements by

$$\alpha_2(t) = \frac{3\langle r^4(t) \rangle}{5(\langle r^2(t) \rangle)^2} - 1. \quad (20)$$

If one assumes that an individual particle motion causes displacements which are distributed by a Gaussian and all such Gaussians have the same width, α_2 should vanish. So if the individual

⁵ Indeed, for the Kohlrausch law (1) such a distribution exists with $g(\tau) > 0$ although it cannot be expressed in closed form. But this is not a strong argument for the ubiquity of the Kohlrausch law because any function which decays completely monotone can be expressed by such a distribution [16].

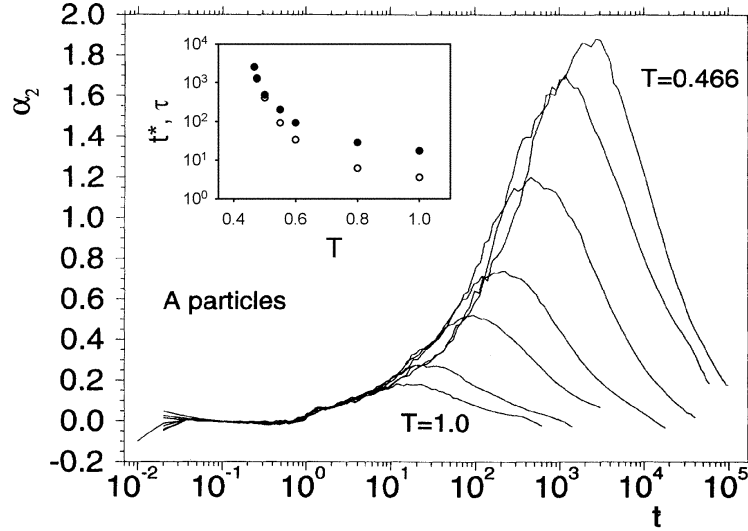


Fig. 9: Non-Gaussian parameter α_2 vs time for the A particles [3]. Temperatures: 1, 0.8, 0.6, 0.55, 0.5, 0.475, 0.466, 0.452, 0.446. The inset show the temperature dependence of the maximum position t^* (full symbols) compared to the relaxation time of the A particle self correlation (hollow symbols).

motions are Gaussian the nGP observed on the whole system should be a direct measure of dynamical heterogeneity, namely

$$\alpha_2 = \left(\frac{\delta \langle r_1^2(t) \rangle}{\langle r_1^2(t) \rangle} \right)^2 \quad (21)$$

where $\delta \langle r_1^2(t) \rangle = \sqrt{\left(\langle r_1^2(t) \rangle - \overline{\langle r_1^2(t) \rangle} \right)^2}$, r_1 is the individual particle displacement, and $\overline{\dots}$ denotes the average over all particles in contrast to $\langle \dots \rangle$ being the thermodynamic average [42]. It has to be noted that there is no reason why the individual particle motion has to be Gaussian and therefore it may be difficult to disentangle an ‘individual’ non-Gaussianity and the effect of dynamical heterogeneity. Nevertheless, the quantity (20) has the advantage that it can be calculated from experiments (neutron scattering, dynamic light scattering, field-gradient NMR) which deliver $F_s(q, t)$.

Already the early simulation results were evaluated in this respect (Fig. 9) and a general picture emerged which could be confirmed by various later works: (i) For short times the nGP vanishes. This is trivial because for a ballistic motion the Maxwell distribution of velocities maps to a Gaussian distribution of displacements. (ii) For long times the nGP vanishes because the motion becomes diffusive and from Fick’s law follows that the distribution of displacements becomes Gaussian. This can also be seen as a consequence of the central limiting theorem. (iii) For intermediate times the nGP can assume considerable values. The maximum grows with decreasing temperature, but it is unclear whether there is a divergence at non-zero temperature. The left wing of the peak in nGP obviously follows a master curve *without* rescaling the time. The maximum position t^* lies in the range of late β /early α relaxation. It shifts with decreasing temperature to longer times but the shift is weaker than for the α relaxation times shown in Fig. 6. It has to be noted that t^* is orders of magnitude large than the ‘first-collision’ time

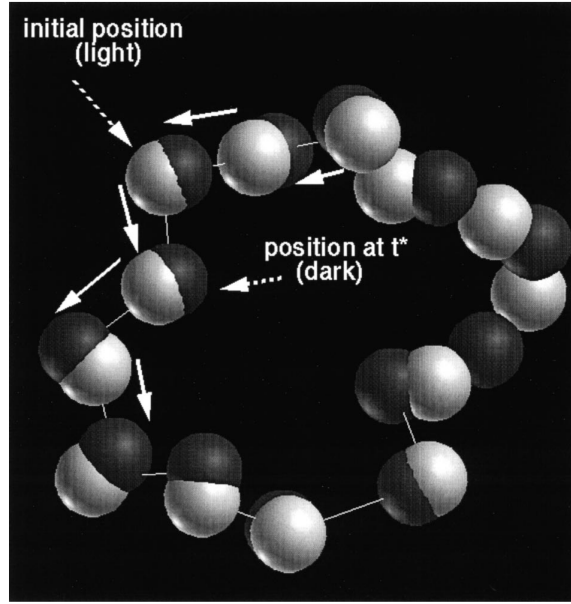


Fig. 10: Loop of 13 particles exhibiting correlated string-like motion at $T = 0.451$. Line segments connect identical particles at successive times. The arrows show the path of some particles [44].

when a particle firstly encounters the effect of caging (about 0.09). This means that the non-Gaussianity is not just a consequence of the ballistic motion being truncated by the cage.

(2) ‘String-like’ cooperative motion. In order to use dynamical heterogeneity as an argument to explain the non-Arrhenius increase of relaxation times in the AG picture another essential property has to be fulfilled: The faster particles have to arrange themselves into clusters (to be identified with the CRRs) rather than being randomly distributed. For that purpose, the (A) particles in the simulation have been classified into ‘mobile’ (about 5%) and ‘less mobile’ according to their instantaneous speed⁶.

‘Visual inspection’ reveals that there are string-like clusters of mobile particles where the particles jump into the positions of their respective neighbours in the string, sometimes even in loops. Such a loop is shown exemplarily in Fig. 10 [44] and its motion can be seen in an animation at [45]. By using a heuristic definition of the position takeover mechanism⁷ it is possible to calculate a length statistics of strings from the simulation results. It turns out that this statistics is approximately exponential. The average string length $\langle n \rangle$ shows an increase when temperature is lowered in agreement with the AG model (Fig. 11).

⁶ This is done by the criterion whether the displacement within time t^* exceeds a certain value r^* . While the definition of t^* is as above the maximum position of the nGP, that of r^* is rather intricate, see [43]. For the qualitative results the details of this definition are not important.

⁷

$$\min (|\mathbf{r}_i(t^*) - \mathbf{r}_j(0)|, |\mathbf{r}_i(0) - \mathbf{r}_j(t^*)|) < 0.6 \quad (22)$$

meaning that within the time span t^* defined by the nGP maximum particle i has taken over the position of particle j or vice versa with an accuracy of 0.6σ . Again the exact definition is not very important for the validity of the results.

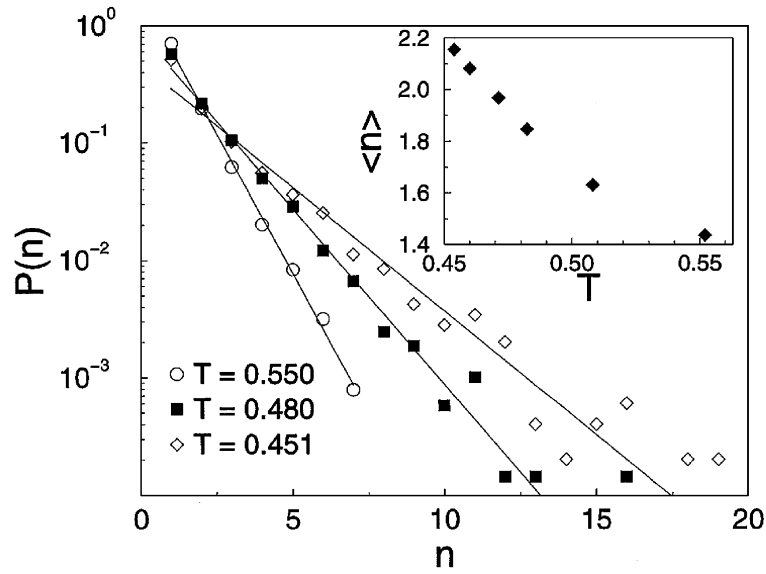


Fig. 11: Probability distribution $P(n)$ of string lengths n for various temperatures. Inset: average $\langle n \rangle$ vs temperature T . [44]

Certain counterarguments to the identification of the strings found here with the CRRs of the AG model should not be concealed: Firstly, the definition of these strings is arbitrary. There is a continuous distribution of jump lengths which does not show a maximum around the next-neighbour distance [48]. This casts some doubt on whether it is possible to extract a population of site-to-site jumps as in a crystal. Secondly, the string-like motion would not show up in collective diffusion but only in self-diffusion. Nevertheless, experiments show that both usually go in parallel in glass forming liquids. Even for the self-motion a loop-like mechanism would be spatially restricted. So the observed long-range diffusion could only be accomplished by successive motions of a particle in several such loops.

Interestingly, similar dynamical structures were found earlier in simulations of a one-component glass⁸ [46]. In these simulations the system is quenched after a short equilibration run to temperatures $\leq 0.15 T_g$. This of course creates a non-equilibrium situation but at such low temperatures the structural relaxation time is virtually infinite and therefore the system is metastable, obtained quantities are again time-translational invariant. Also, the real experiment is not in a qualitatively better position: The cooling rate may be slower but inevitably also the real samples upon cooling fall out of equilibrium close to T_g . The first computer experiments were done in order to identify a common anomaly in the vibrational spectrum of glasses, the so-called boson peak [47]. For this purpose diagonalisation of the force constant matrix was done for the glassy structure [49]. In addition to the spectrum (which indeed shows the same anomaly as found in experiments on real glasses), the eigenvectors can be calculated from the simulation. In that way the information was obtained that the anomalous vibrational modes are localised to about ten particles and that these particles are arranged in string-like clusters apparently similar to those found in the liquid [50]. Interestingly, at higher temperatures (but still far below the glass temperature, $T \leq 0.15 T_g$) the same clusters exhibit local relaxations [51]. The jumps associated with this relaxation are much smaller than those described above for the liquid, namely only

⁸ Note that all results hitherto presented correspond to temperatures $T > T_c > T_g$, i.e. in the equilibrium liquid.

a fraction of the next neighbour distance. Also the temperature at which the relaxation is observed is so low that they cannot be identified with the α relaxation. Nevertheless, the similarity is striking and the question arises whether there is any relation between the string-like clusters in the glass and those in the liquid. Of course, it is currently difficult to tackle this question in consideration of the gap $(0.15 T_g \dots 1.2 T_g)$ between the two types of computer experiments.

(3) Four-point correlators. The previously described procedure to identify dynamical heterogeneities is usually called ‘subset approach’ [52] because by some criterion of ‘mobility’ the faster (or slower) particles are sorted out. It suffers somewhat from the arbitrariness of that criterion. A more general approach is that of the definition of new correlators. To explain this firstly the density-density correlation function in *real* space is recalled here:

$$\begin{aligned} G(\mathbf{r}, t) &= \left\langle \int d^3 r' (\varrho(\mathbf{r} + \mathbf{r}', t) - \langle \varrho \rangle) (\varrho(\mathbf{r}', 0) - \langle \varrho \rangle) \right\rangle \quad \text{where} \\ \varrho(\mathbf{r}, t) &= \sum_i \delta(\mathbf{r}_i(t) - \mathbf{r}). \end{aligned} \quad (23)$$

The Fourier transform of this quantity to reciprocal (q) space gives the numerator of (17). The special static ($t = 0$) case of this correlator is

$$\begin{aligned} G(\mathbf{r}) &= \left\langle \int d^3 r' (\varrho(\mathbf{r} + \mathbf{r}') - \langle \varrho \rangle) (\varrho(\mathbf{r}') - \langle \varrho \rangle) \right\rangle \quad \text{where} \\ \varrho(\mathbf{r}) &= \sum_i \delta(\mathbf{r}_i - \mathbf{r}). \end{aligned} \quad (24)$$

Here, Fourier transform gives the denominator of (17), the structure factor $S(q)$. This is also the quantity which is observed in a diffraction experiment. This correlator is now modified in a way that the δ functions belonging to more mobile particles are weighted more strongly:

$$\begin{aligned} G_u(\mathbf{r}, \Delta t) &= \left\langle \int d^3 r' (u(\mathbf{r} + \mathbf{r}', \Delta t) - \langle u \rangle) (u(\mathbf{r}', \Delta t) - \langle u \rangle) \right\rangle \quad \text{where} \\ u(\mathbf{r}, \Delta t) &= |\mathbf{r}_i(\Delta t) - \mathbf{r}_i(0)| \sum_i \delta(\mathbf{r}_i - \mathbf{r}). \end{aligned} \quad (25)$$

Note that the meaning of Δt in (25) and t in (23) is completely different. While the latter is a time offset between the structures to be correlated, the former is a ‘development’ time applied to each of the structures to be correlated. There are several experimental methods to measure the correlator (23) but currently none for (25). So computer simulation is the only way to access this ‘displacement-displacement correlator’.

If one compares the concept of (25) with that of (23) one notes that the displacement correlator involves four positions of the particles considered, namely $\mathbf{r}_1(0)$, $\mathbf{r}_1(\Delta t)$, $\mathbf{r}_2(0)$, and $\mathbf{r}_2(\Delta t)$. Therefore, it is a special case of a four-point correlator in contrast to (23) which only involves two points, namely $\mathbf{r}_1(0)$ and $\mathbf{r}_2(t)$. Indeed, the simplest density correlation function that contains information on correlated particle motion is fourth-order [53]. Therefore, it is another natural approach to study the *general* four-point correlation function

$$\begin{aligned} G_4(\mathbf{r}_1, \mathbf{r}_2, \mathbf{r}_3, \mathbf{r}_4, t) &= \langle \varrho(\mathbf{r}_1, 0) \varrho(\mathbf{r}_2, t) \varrho(\mathbf{r}_3, 0) \varrho(\mathbf{r}_4, t) \rangle \\ &\quad - \langle \varrho(\mathbf{r}_1, 0) \varrho(\mathbf{r}_2, t) \rangle \langle \varrho(\mathbf{r}_3, 0) \varrho(\mathbf{r}_4, t) \rangle. \end{aligned} \quad (26)$$

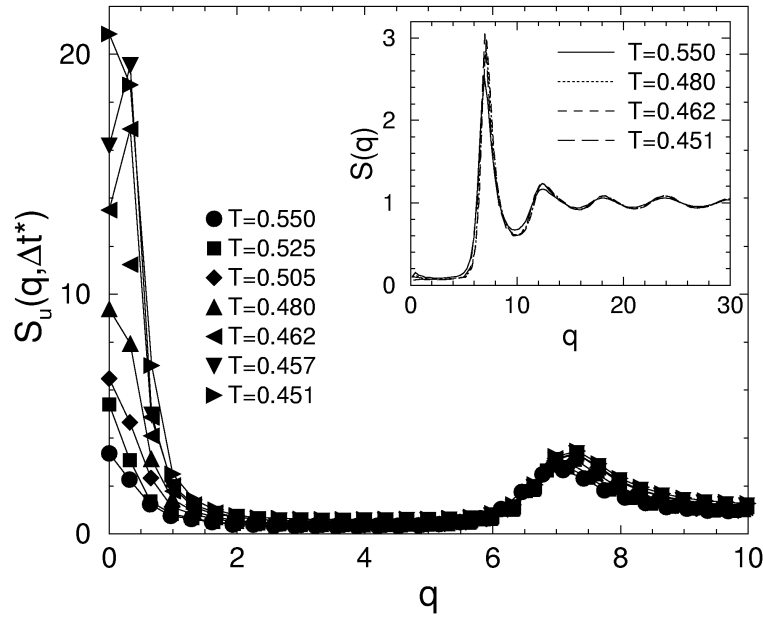


Fig. 12: $S_u(q, \Delta t^*)$ versus q for different temperatures. (Δt^* is the time span where $S_u(0, \Delta t^*)$ reaches its maximum.) Inset: static structure factor $S(q)$ for some of the temperatures. [56].

Actually, the results from evaluation of this correlator [53, 54] are not much different from those using the more evident displacement correlator [55, 52, 56]. Therefore only the results from the latter will be presented here.

Fig. 12 shows the Fourier transform $S_u(q, \Delta t^*)$ of the displacement correlator (25). The time span Δt^* is chosen so that $S_u(0, \Delta t^*)$ (which is related to the integral of $G_u(q, \Delta t^*)$) reaches a maximum. It can be seen that for high q this ‘displacement structure factor’ is not much different from the ordinary $S(q)$. But for small q a strong peak develops around $q = 0$ indicating long range dynamical correlations. These correlations obviously do not have any effect on the static structure factor $S(q)$ what explains that they could not be observed in the numerous diffraction experiments on glass forming liquids. Later studies were able to identify a correlation length $\xi_{\text{corr}}(T)$ which strongly increases upon cooling [54] as expected in the AG framework.

2.4 Confinement effects

An approach often used in experiment to identify the length scale involved in the glass transition is that of *confinement* [57, 58]. The idea behind such experiments is that as soon as the length $\xi(T)$ exceeds the size of a small volume of a glass former its properties should become different from those of the bulk material. The results of such experiments often seem contradicting. There is even no agreement about the question whether T_g is decreased or increased by confinement [57], i.e. whether confinement accelerates or decelerates the α relaxation.

In addition it is often difficult to prepare systems with the appropriate confinement size usually in the nanometre range. On the first glance this seems no difficulty for computer simulation because it just means a change of the boundary conditions. Nevertheless, there is a problem associated with simply replacing the walls of the simulation box with repulsive walls: These walls create a layering of the liquid which may not be so pronounced in a real experiment where the walls are rough on an atomic length scale.

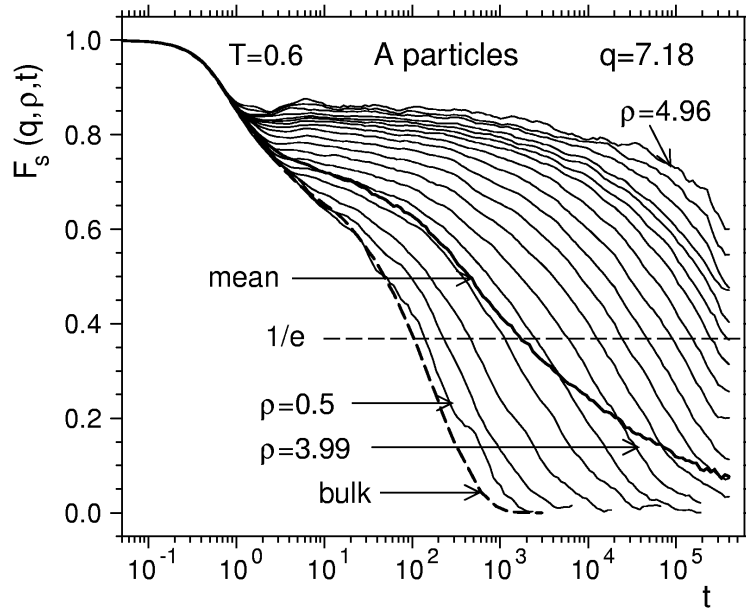


Fig. 13: Time dependence of the position dependent self-correlation function $F_s(q, \rho, t)$ for various distances ρ [59]. The thick solid curve and the dashed solid curves are the intermediate scattering function for the whole system and the bulk system, respectively.

A computational trick to construct a rough wall avoiding this effect is the following [59]: After the equilibration run, the particles beyond a defined pore surface are ‘frozen’, i.e. their coordinates are kept constant. The time evolution is only calculated for the remaining particles. In that way it can be assured that the structure is only minimally affected because the wall consists of particles of the same kind and same structure as the liquid⁹.

Fig. 13 shows the self-correlation function (18) calculated from such a simulation in a cylindrical pore of radius 5σ (corresponding to about 3.5 nm diameter) [61]. (Except for the confinement all parameters are chosen as in the previous section.) One can see that the relaxation in the pore (solid curve) is clearly slower than that of the bulk (dashed curve). It is also obvious that the relaxation is more ‘stretched’, i.e. the parameter β of the Kohlrausch law (1) would have to be very small if such a fit would even be possible.

Computer simulation now allows to analyse this behaviour in more depth. One can define a position dependent self-correlation function

$$F_s(q, \rho, t) = \left\langle \sum_i \delta(\rho_i(0) - \rho) \exp(i\mathbf{q} \cdot (\mathbf{r}_i(t) - \mathbf{r}_i(0))) \right\rangle \quad (27)$$

where $\rho_i = \sqrt{x_i^2 + y_i^2}$ is the distance from the central axis of the pore. This function only considers particles which have the same distance to the wall at time zero. In Fig. 13 $F_s(q, \rho, t)$ for various values of ρ is added. Obviously, the relaxation time has a strong dependence on the position of the particles. It is orders of magnitude slower at the walls than at the centre of the pore. The dynamics is strongly heterogeneous but here the heterogeneity is *extrinsic* in addition to the intrinsic heterogeneity discussed in the last section. Although the individual $F_s(q, \rho, t)$

⁹ With the same objective a liquid-crystal interface can be used [60]. During the time span of the simulation this interface does not ‘melt away’.

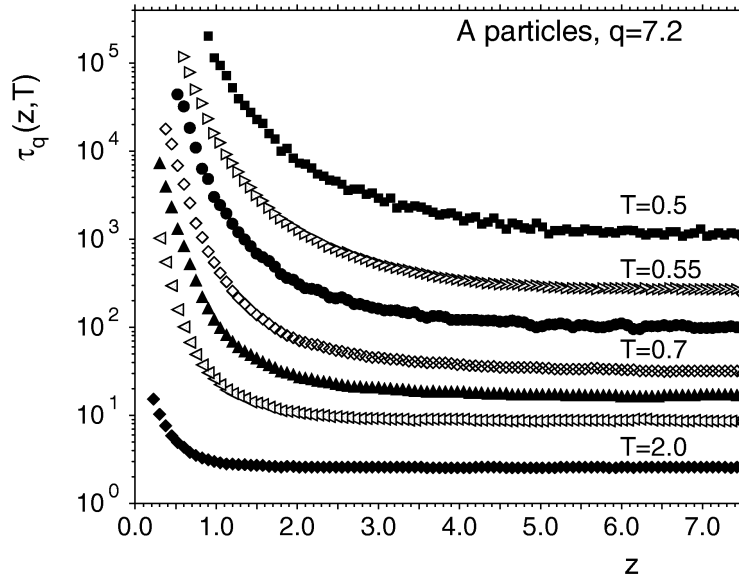


Fig. 14: z dependence of the relaxation time for different temperatures [61] ($T = 2.0, 1.0, 0.8, 0.7, 0.6, 0.55, 0.5$). The open diamonds on the right are the values for the bulk.

have about the same shape as the bulk $F_s(q, t)$ the averaging over all particles results in the dramatic stretching of $F_s(q, t)$ in the confined situation.

This is an important finding which has to be considered in the evaluation of real experiments where one usually measures such an average. Often experimental data is not treated as resulting from heterogeneous dynamics. This may explain that, depending on the average realised in the experiment, different outcomes of the confinement effect are reported (acceleration, deceleration, or no change).

The dependence of the relaxation time (defined as usual as the $1/e$ time) is depicted in Fig. 14 for a similar simulation but in a confined *film* [61]. Close to the wall the relaxation time increases strongly with decreasing distance z and can be fitted by a double-exponential,

$$\ln(\tau(z)/\tau_{\text{bulk}}) \propto \exp(-z/\xi_{\text{wall}}(T)). \quad (28)$$

The fact that this expression fits shows that in the limit of large distance from the wall the relaxation becomes bulk-like. This can also be estimated directly from Figs. 14 or 13. This behaviour is what one would expect intuitively. Nevertheless, real experiments often show that the distribution of relaxation times has faster components than in the bulk or even has an average faster than the bulk [62, 63]. The simulation results cannot reproduce this acceleration effect for rough walls.

Expression (28) also defines a characteristic length $\xi_{\text{wall}}(T)$ which is about the same as the size of the mobile clusters ($\xi_{\text{corr}}(T)$) observed in the studies reported in the last section. This suggests an explanation based on a blocking of the cooperative motion when the clusters touch the wall.

Interestingly, mathematically smooth walls have just the opposite effect, namely an acceleration of relaxation close to the wall [61]¹⁰. This can be explained by particles which use the less

¹⁰ In this study the structural distortion by the smooth wall was suppressed by introducing an additional multi-particle force.

structured potential of the wall to bypass the barrier between the potential minima created by their neighbouring particles. Although the effect on the average is not so pronounced there, for smooth walls one would expect a faster average relaxation. But one has to note that, except for systems like free-standing polymer films, this is not the real experimental situation. And even the free-standing film would correspond to a somewhat different situation, namely a force-free surface.

3 Summary

From the exemplary studies presented here, two aspects can be seen where computer simulation is of importance for the study of glass forming systems:

(1) Construction of ideal systems. Although on the first glance it may seem a drawback of computer simulation that systems have to be ‘oversimplified’ to perform viable simulations over long times, with respect to theories such as MCT, this can also be seen as an advantage. Often such theories focus on the ‘universal’ behaviour of glass formers and do not include dynamic processes as secondary relaxations (i.e. those of molecular side groups). On the other hand in real samples a certain molecular complexity is inevitable to avoid crystallisation. With computer simulation one can come much closer e.g. to the ‘MCT fluid’ consisting of structureless particles.

Another advantage is that boundary conditions can be imposed freely. The ‘mathematically smooth walls’ described in the last section certainly cannot be realised in experiment. Even the situation of rough surfaces is difficult to prepare on a nanoscopic length scale and it cannot be avoided to construct the walls from a different material as the confined liquid.

(2) Observation of microscopic variables. Computer simulation generates the full trajectory of the system, i.e. the positions and velocities of all particles at all times. No experimental method is able to do so for an atomistic system¹¹. Of course, it is possible to measure certain correlators, e.g. the density correlation functions (17) and (18) by inelastic neutron scattering. But these methods are usually restricted to two-point correlators or as is the case for multidimensional NMR do not measure density correlators.

With respect to confined glass forming systems computer simulation offers the important opportunity to extract position dependent correlators. In this way, the dependence of the dynamics on the distance from the confining wall can be studied. This is usually not possible in real experiments where an average over all particles is measured.

A current weakness of computer simulation (in comparison to real experiments) is its restriction in the time range. While macroscopic experiments can be done without problems on the scale of days, computer simulation currently struggles to reach the microsecond scale. This concerns the simulation run time as well as the preceding equilibration. The consequence of this is that most of the simulations today are done in the temperature region $T > T_c \approx 1.2T_g$. But just the region $T_g \dots T_c$ is very interesting because there one expects (and observes in the experiment) deviations from ideal MCT behaviour.

There is currently not much prospect that this situation can be resolved by improving programming techniques [65]. The equilibration problem may be solved by techniques which involve

¹¹ By confocal microscopy it is possible to obtain this full information for colloidal glasses [64]. These are model systems where the atoms are replaced by colloidal particles about a thousand times bigger.

an unphysical (faster) propagation of the system before the simulation with the actual ‘physical’ algorithm is started, e.g. ‘parallel tempering’ [66] or the ‘slithering snake algorithm’ for polymers [67]. Nevertheless, the problem that the correlators itself have to be calculated over an enormous number of time steps remains.

On the other hand, the computation power of computers increases until now more than exponentially [68]. There are still about six decades to surmount until times up to one second (being the relaxation time at T_g) can be simulated in a Lennard-Jones system¹². Depending on whether one extrapolates exponentially using the current time constant or uses the more ‘optimistical’ Kurzweil prediction [68] this will be possible in 10–25 years.

Acknowledgement

The author thanks Herbert Schober for critical reading which helped to make the manuscript a lot more understandable.

¹² To compare, there are about eight decades until the human brain can be simulated in real time.

References

- [1] Donth E 2001 *The glass transition: relaxation dynamics of liquids and disordered materials* (Berlin: Springer)
- [2] Anderson P W 1995 *Science* **267** 1615
- [3] Kob W and Andersen H C 1995 *Phys. Rev. E* **51** 4626
- [4] Baschnagel J 1993 *Physica A* **201** 157
- [5] Kohlrausch R 1854 *Ann. Phys. (Leipzig)* **91** 56
- [6] Zorn R, McKenna G B, Willner L, and Richter D 1995 *Macromolecules* **28** 8552
- [7] Fytas G and Ngai K L 1988 *Macromolecules* **21** 804
- [8] Richter D, Frick B, and Farago B 1988 *Phys. Rev. Lett.* **61** 2465
- [9] Götze W 1991 *Aspects of Structural Glass Transition* eds Levesque D, Zinn-Justin J, and Hansen J P (Amsterdam: North Holland) p 289
- [10] Götze W and Sjögren L 1987 *J. Phys. C* **20** 879
- [11] Ngai K L 1994 *Disorder Effects on Relaxational Properties* eds Richert R and Blumen A (Berlin: Springer) p 89 and references therein
- [12] Roy A K and Blumen A 1989 *J. Chem. Phys.* **91** 4353
- [13] Shlesinger M F 1988 *Ann. Rev. Phys. Chem.* **39** 269
- [14] Palmer R G, Stein D L, Abrahams E, and Anderson P W 1984 *Phys. Rev. Lett.* **53** 958
- [15] Flesselles J-M and Botet R 1988 *J. Phys. A* **22** 903
- [16] Feller W 1971 *An Introduction to Probability Theory* (New York: Wiley)
- [17] Angell C A 1984 *Relaxations in Complex Systems* eds Ngai K L and Wright G B (Springfield: National Technical Information Service) p 3
- [18] Angell C A and Sichina W 1967 *Ann. NY Acad. Sci.* **279** 53
Angell C A 1988 *J. Phys. Chem. Solids* **49** 863
- [19] Oldekop W 1956 *Glastechn. Ber.* **30** 8
- [20] Vogel H 1921 *Physik. Zeitschr.* **22** 645
- [21] Fulcher G F 1925 *J. Am. Ceram. Soc.* **8** 339
- [22] Edgeworth R, Dalton B J and Parnell T 1984 *Eur. J. Phys.* **5** 198
- [23] O'Connell P A and McKenna G B 1999 *J. Chem. Phys.* **110** 11054
- [24] Stickel F, Fischer E W, and Richert R 1995 *J. Chem. Phys.* **102** 6251

- [25] Stickel F, Fischer E W, and Richert R 1995 *J. Chem. Phys.* **104** 2043
Hansen C, Stickel F, Richert R, and Fischer E W 1998 *J. Chem. Phys.* **108** 6408
- [26] Böhmer R, Ngai K L, Angell C A, and Plazek D J 1993 *J. Chem. Phys.* **99** 4201
- [27] Ngai K L 2000 *J. Phys.: Condensed Matter* **12** 6437
- [28] Ferry J D 1980 *Viscoelastic Properties of Polymers* (New York: John Wiley & Sons)
- [29] Zorn R, Mopsik F I, McKenna G B, Willner L, and Richter D 1997 *J. Chem. Phys.* **107** 3645
- [30] Berry G C and Fox T G 1968 *Adv. Polym. Sci.* **5** 261
- [31] Götze W and Sjögren L 1988 *J. Phys. C* **21** 3407
- [32] Johari G P and Goldstein M 1970 *J. Chem. Phys.* **53** 2372
- [33] von Schweidler E 1907 *Ann. Phys.* **24** 711
- [34] Adam G and Gibbs J H 1965 *J. Chem. Phys.* **43** 139
- [35] Richert R 2002 *J. Phys.: Condens. Matter* **14** R703
- [36] Kob W and Andersen H C 1994 *Phys. Rev. Lett.* **73** 1376
- [37] Kob W and Andersen H C 1995 *Phys. Rev. E* **52** 4134
- [38] Fuchs M 1994 *J. Non-Cryst. Solids* **172–174** 241
Fuchs M and Latz A 1993 *Physica A* **201** 1
- [39] Nauroth M and Kob W 1997 *Phys. Rev. E* **55** 657
- [40] Gleim T and Kob W 2000 *Eur. Phys. J. B* **13** 83
- [41] Rahman A, Singwi K S and Sjölander A 1962 *Phys. Rev.* **126** 986
Rahman A 1964 *Phys. Rev.* **136** A405
- [42] Zorn R 1997 *Phys. Rev. B* **55** 6249
- [43] Kob W, Donati C, Plimpton S J, Poole P H and Glotzer S C 1997 *Phys. Rev. Lett.* **79** 2827
- [44] Donati C, Douglas J F, Kob W, Plimpton S J, Poole P H and Glotzer S C 1998 *Phys. Rev. Lett.* **80** 2338
- [45] <http://www.ctcms.nist.gov/~donati/movie.html>
- [46] Schober H R, Oligschleger C and Laird B B 1993 *J. Non-Cryst. Solids* **156–158** 965
- [47] *Amorphous Solids: Low Temperature Properties* ed Phillips W A (Springer: Berlin) 1981
- [48] Kluge M and Schober H R 2004 *Phys. Rev. B* **70** 224209
- [49] Laird B B and Schober H R 1991 *Phys. Rev. Lett.* **66** 636
Schober H R and Laird B B 1991 *Phys. Rev. B* **44** 6746

- [50] Schober H R and Oligschleger C 1996 *Phys. Rev. B* **53** 11469
- [51] Oligschleger C and Schober H R 1999 *Phys. Rev. B* **59** 811
- [52] Glotzer S C and Donati C 1999 *J. Phys.: Condens. Matter* **11** A285
- [53] Glotzer S C, Novikov V N and Schrøder T B 2000 *J. Chem. Phys.* **112** 509
- [54] Lačević N, Starr F W, Schrøder T B and Glotzer S C 2003 *J. Chem. Phys.* **119** 7372
Lačević N and Glotzer S C 2003 *J. Phys.: Condens. Matter* **15** S2437
- [55] Poole P H, Donati C and Glotzer S C 1998 *Physica A* **261** 51
- [56] Donati C, Glotzer S C and Poole P H 1999 *Phys. Rev. Lett.* **82** 5064
- [57] Alcoutlabi M and McKenna G B 2005 *J. Phys.: Condens. Matter* **17** R461
- [58] Frick B, Alba-Simionesco, Dosseh G, LeQuellec C, Moreno A J, Colmenero J, Schönhals A, Zorn R, Chrissopoulou K, Anastasiadis S H and Dalnoki-Verres K 2005 *J. Non-Cryst. Solids* **351** 2657
- [59] Scheidler P, Kob W and Binder K 2000 *J. Phys. IV France* **10** Pr7-33
Scheidler P, Kob W and Binder K 2000 *Europhys. Lett.* **52** 277
- [60] Teichler H, unpublished
- [61] Scheidler P, Kob W and Binder K 2003 *Eur. Phys. J. E* **12** 5
- [62] Arndt M, Stannarius R, Groothues H, Hempel E and Kremer F 1997 *Phys. Rev. Lett.* **79** 2077
- [63] Zorn R, Hartmann L, Frick B, Richter D and Kremer F 2002 *J. Non-Cryst. Solids* **307–310** 547
- [64] Weeks E R, Crocker J C, Levitt A C, Schofield A and Weitz D A 2000 *Science* **287** 627
- [65] Binder K, Baschnagel J, Kob W and Paul W 2002 *Bridging Time Scales: Molecular Simulations for the Next Decade* eds Nielaba P, Mareschal M and Ciccotti G (Berlin: Springer) p 199
- [66] Hansmann U H E and Okamoto Y 1999 *Annu. Rev. Comp. Phys.* **VI** 179
Iba Y 2001 *J. Mod. Phys. C* **12** 623
- [67] Wolfgardt M, Baschnagel J and Binder K *J. Phys. II France* **5** 1035
- [68] <http://www.kurzweilai.net>